



Review of a direct epitaxial approach to achieving micro-LEDs

Yuefei Cai(蔡月飞), Jie Bai(白洁), and Tao Wang(王涛)

Citation: Chin. Phys. B, 2023, 32 (1): 018508. DOI: 10.1088/1674-1056/ac90b5

Journal homepage: <http://cpb.iphy.ac.cn>; <http://iopscience.iop.org/cpb>

What follows is a list of articles you may be interested in

Interface effect on superlattice quality and optical properties of InAs/GaSb type-II

superlattices grown by molecular beam epitaxy

Zhaojun Liu(刘昭君), Lian-Qing Zhu(祝连庆), Xian-Tong Zheng(郑显通), Yuan Liu(柳渊), Li-Dan Lu(鹿利单), and Dong-Liang Zhang(张东亮)

Chin. Phys. B, 2022, 31 (12): 128503. DOI: 10.1088/1674-1056/ac8729

A 4×4 metal-semiconductor-metal rectangular deep-ultraviolet detector array of

Ga₂O₃ photoconductor with high photo response

Zeng Liu(刘增), Yu-Song Zhi(支钰崧), Mao-Lin Zhang(张茂林), Li-Li Yang(杨莉莉), Shan Li(李山), Zu-Yong Yan(晏祖勇), Shao-Hui Zhang(张少辉), Dao-You Guo(郭道友), Pei-Gang Li(李培刚), Yu-Feng Guo(郭宇锋), and Wei-Hua Tang(唐为华)

Chin. Phys. B, 2022, 31 (8): 088503. DOI: 10.1088/1674-1056/ac597d

Micro-light-emitting-diode array with dual functions of visible light communication and illumination

Yong Huang(黄涌), Zhi-You Guo(郭志友), Hui-Qing Sun(孙慧卿), Hong-Yong Huang(黄鸿勇)

Chin. Phys. B, 2017, 26 (10): 108504. DOI: 10.1088/1674-1056/26/10/108504

Chemical synthesis of zinc oxide nanorods for enhanced hydrogen gas sensing

Musarrat Jabeen, Muhammad Azhar Iqbal, R Vasant Kumar, Mansoor Ahmed, Muhammad Tayyeb Javed

Chin. Phys. B, 2014, 23 (1): 018504. DOI: 10.1088/1674-1056/23/1/018504

Recent progress in perpendicularly magnetized Mn-based binary alloy films

Zhu Li-Jun(朱礼军), Nie Shuai-Hua(聂帅华), Zhao Jian-Hua(赵建华)

Chin. Phys. B, 2013, 22 (11): 118505. DOI: 10.1088/1674-1056/22/11/118505

Review of a direct epitaxial approach to achieving micro-LEDs

Yuefei Cai(蔡月飞)^{1,†}, Jie Bai(白洁)², and Tao Wang(王涛)^{2,‡}

¹Department of Electronic and Electrical Engineering, Southern University of Science and Technology, Shenzhen 518055, China

²Department of Electronic and Electrical Engineering, The University of Sheffield, Sheffield S1 3JD, United Kingdom

(Received 30 July 2022; revised manuscript received 30 August 2022; accepted manuscript online 9 September 2022)

There is a significantly increasing demand of developing augmented reality and virtual reality (AR and VR) devices, where micro-LEDs (μ LEDs) with a dimension of $\leq 5 \mu\text{m}$ are the key elements. Typically, μ LEDs are fabricated by dry-etching technologies, unavoidably leading to a severe degradation in optical performance as a result of dry-etching induced damages. This becomes a particularly severe issue when the dimension of LEDs is $\leq 10 \mu\text{m}$. In order to address the fundamental challenge, the Sheffield team has proposed and then developed a direct epitaxial approach to achieving μ LEDs, where the dry-etching technologies for the formation of μ LED mesas are not needed anymore. This paper provides a review on this technology and then demonstrates a number of monolithically integrated devices on a single chip using this technology.

Keywords: micro-LED, epitaxial growth, gallium nitride, display

PACS: 85.60.Jb, 81.16.-c, 81.05.Ea

DOI: 10.1088/1674-1056/ac90b5

1. Introduction

With the advent of “5G era” which is expected to penetrate into every aspect of our daily life, a number of new optoelectronics will have to be developed to meet a wide range of applications, such as augmented reality and virtual reality (AR and VR) devices, microdisplays for smartphones and smart-watches, autodisplay, next generation TV, where III-nitride based micro light-emitting diodes (μ LEDs) are the key components.^[1–4] AR & VR micro-displays which require μ LEDs with ultra-small dimensions are typically utilized in small spaces or at close proximity to the eye. Therefore, such a microdisplay needs to exhibit high resolution, high contrast ratio, high luminance, high external quantum efficiency (EQE) and narrow spectral linewidth. Yole Développement has predicted that the global microdisplay market will reach \$4.2 billion by 2025 at a compound annual growth rate (CAGR) of 100%.

The III-nitride μ LEDs demonstrate many unique advantages over either organic LEDs (OLEDs) or liquid crystal displays (LCDs). For example, III-nitride based microdisplays, where μ LEDs are the essential components and are self-emissive, exhibit much higher resolution, higher efficiency, and higher contrast ratio than either OLEDs or LCDs. Furthermore, III-nitride μ LEDs display much longer operation lifetime and much stronger chemical robustness than either OLEDs or LCDs.^[1–4] Generally speaking, μ LEDs with a dimension of $\leq 100 \mu\text{m}$ are typically used for the fabrication of autodisplay and next-generation TV, while AR/VR devices require μ LEDs with a dimension of $\leq 5 \mu\text{m}$. In addition,

ultra-small μ LEDs exhibit significantly reduced junction capacitance due to their physical dimension, which is crucial for achieving a high-speed data transmission rate with a GHz modulation bandwidth that is necessary for visible light communication (VLC) applications.^[5,6]

So far, III-nitride μ LEDs are basically fabricated by using standard photolithography techniques and dry-etching processes.^[7–12] It is well-known that dry-etching processes unavoidably bring substantial damages to the surface and the sidewalls of LEDs, which enhance non-radiative recombination leading to reduction in optical performance.^[13–18] This may be a minor issue and can be negligible in the case of the fabrication of standard LEDs with a dimension of $\geq 100 \mu\text{m}$. However, this issue cannot be ignored anymore when the dimension of μ LEDs decreases down to the tens micrometer scale and eventually becomes a major factor which is responsible for severe degradation in optical performance.^[14,15,19] To be more specific, it is necessary to comment three major challenges which conventional dry-etching methods are facing before a proposed idea can be put forward.

Drying etching processes such as inductively coupled plasma (ICP) dry etching techniques have been widely used to define either broad area LED mesas or μ LED mesas in the semiconductor industry. As stated above, dry-etching technologies unavoidably lead to a significant reduction in the quantum efficiency of μ LED compared with large area LEDs. Although the passivation technology has been used aiming to reduce plasma induced damages on the sidewalls of μ LEDs during dry-etching processes, the improvement is marginal

[†]Corresponding author. E-mail: caiyf@sustech.edu.cn

[‡]Corresponding author. E-mail: t.wang@sheffield.ac.uk

even if an advanced atomic layer deposition (ALD) technique is used instead of a standard plasma-enhanced chemical vapor deposition (PECVD) technique.^[14] This passivation procedure also generates an extra issue, namely, the etching back of the dielectric layer on top of the p-contact/p-GaN of μ LEDs, potentially degrading electrical injection in the p-GaN region.^[13] This becomes particularly challenging for the fabrication of ultra-small μ LEDs, such as μ LEDs with a dimension of $\leq 5 \mu\text{m}$. Consequently, the EQE of the μ LEDs with a dimension of $\leq 5 \mu\text{m}$ is very low and is limited to 1% to 5%, meaning that such μ LEDs cannot meet the requirement for AR/VR applications. Very recently, it has been reported that severe damage on the sidewalls of the μ LEDs has been clearly observed on blue μ LEDs with a dimension of $\leq 5 \mu\text{m}$ in a square shape.^[20] This also means that it is extremely challenging to apply the conventional fabrication approaches which mainly combine a standard photolithography technique and subsequent dry-etching processes in obtaining ultra-small μ LEDs with satisfied performance.

Conventional III-nitride LEDs exhibit a broad spectral linewidth due to the nature of InGaN alloys which are used as an emitting region. A significant reduction in the spectral linewidth of μ LEDs is necessary for achieving microdisplays with high resolution especially for AR and VR. Generally, InGaN LEDs exhibit an intrinsically broad spectral linewidth mainly due to indium segregation and alloy fluctuation. This becomes more severe with increasing emission wavelength, as higher indium content InGaN is required to obtain a longer emission wavelength. It is necessary to develop a new approach or process to overcome the fundamental limitations, allowing us to not only further increase the EQE of μ LEDs but also significantly reduce their spectral line width.

Currently, it is naturally difficult to achieve III-nitride μ LEDs with a long-wavelength emission, such as red emission which is one of the three fundamental components for the formation of RGB (red, green, blue) based full color display. So far, InGaN-based μ LEDs with reasonably good performance in the blue and green spectral region have been reported. However, it is very challenging to achieve higher indium content InGaN to extend the emission wavelengths beyond the green spectral region while maintaining high optical performance.^[21,22] A typical method to achieve higher indium content in InGaN is to lower the growth temperature for InGaN, but this method is not ideal because it is expected that a reduction in growth temperature generally causes a significant degradation in crystal quality. In general, vapor–solid thermodynamic equilibrium can be modified by stress, making the solid-phase epitaxial composition reduce toward lattice-matched conditions. This is the major reason why it is so difficult to enhance indium incorporation into GaN.^[23–32] Therefore, the growth of InGaN on a relaxed layer is beneficial for

obtaining high indium content in InGaN. However, it is worth highlighting that the formation of a relaxed layer is often associated with the generation of extra defects if a heterostructure with a large lattice mismatch is used to generate the relaxed layer. This leads to degradation in optical performance. Inserting a thin AlN or an AlGaN layer into each InGaN quantum well as an emitting region leads to an enhancement in strain that pushes the emission wavelength of InGaN quantum wells toward longer wavelength.^[30,31] So far, this approach has become a popular method for the growth of red LEDs,^[27–32] but leading to a reduction in the internal quantum efficiency.

Therefore, it is necessary to develop a game-changing approach to the growth and then the fabrication of μ LEDs to address all the challenges discussed above. In addition, any new approaches will have to be simplified and scalable to meet industrial requirements in terms of mass-production.

2. Nature and mechanism of the confined selective epitaxy approach

To address the challenges mentioned above, the Sheffield team has proposed and then developed a direct epitaxy approach which we call the “confined selective epitaxy” (CSE) approach^[33,34] This direct epitaxy approach is different from either homoepitaxy or heteroepitaxy approach. This is also different from any conventional selective epitaxy approaches. For any conventional selective epitaxy approaches, epitaxial growth is initially carried out within an area which is formed by thin dielectric masks until the growth is above the masks and then epitaxial growth carries on in an unconfined manner along both the vertical direction and the lateral direction. In contrast, for our proposed CSE approach, epitaxial growth is always conducted within a confined area throughout the whole epitaxial growth process. Therefore, the growth mechanism of our CSE approach is entirely different from any conventional selective epitaxy approaches because the masks always confine the epitaxy growth and thus significantly affect the deposition of the epitaxial layers. Furthermore, if the confined area for CSE is smaller, the non-uniformity of atomic deposition becomes more severe. Therefore, it is crucial to develop a new growth procedure to effectively suppress atomic deposition in a non-uniform manner during the whole epitaxial growth processes, which is the key to achieve CSE successfully. Of course, the CSE approach allows either photonics or electronics to be naturally formed on a micrometer scale as long as the predefined masks used are on the micrometer scale, meaning that dry etching is not required for the fabrication of μ LED mesas (the 1st step for the fabrication of any semiconductor device) anymore. It means the physical dimension of a device is essentially determined by the dimensions of the predefined masks used for CSE. Therefore, there is no plasma

induced damage which always exists during conventional dry-etching processes. In principle, unlike either homoepitaxy or heteroepitaxy approach, the CSE approach does not necessarily rely on a substrate used. Another advantage of our CSE is that it is easy to achieve an on-chip monolithic integration of optoelectronics and electronics, where of course no dry-etching is needed anymore. Based on our CSE approach, the Sheffield team has achieved ultra-small μ LEDs without involving dry-etching processes, leading to the demonstration of ultra-small and ultra-compact μ LEDs with a record EQE and small reverse leakage current in the green and red spectral regions.^[33,34,36,37] Based on this CSE approach, by epitaxially integrating a microcavity and ultra-small μ LEDs, ultra-small and ultra-compact μ LEDs with a stabilized emission wavelength have been achieved,^[35] which is extremely important for practical applications and has addressed the long-standing issue in the field of III-nitride optoelectronics. In addition, the CSE approach has also been employed to monolithically integrate μ LEDs with high electron mobility transistors (HEMTs) for visible light communication (VLC) and display applications.^[38,39]

3. The CSE approach

3.1. Demonstration of ultra-small μ LEDs

For our CSE approach, the first step is to form a selective growth mask on a template, where subsequent epitaxial growth can be carried out in a confined manner throughout the whole growth process. In order to ensure entirely confined selective epitaxial growth, a mask will have to be properly designed and then fabricated in terms of the parameters required for CSE such as sidewalls and thickness. In principle, the used template for CSE can be any structure, either a single GaN on sapphire or silicon or any other substrate, or an epitaxial distributed Bragg reflector (DBR) structure on sapphire or silicon or any other substrate, or a high electron mobility transistor structure on sapphire or silicon or any other substrate, or any other epitaxial layer. For a demonstration purpose, a standard single n-GaN on sapphire is used as a template, on which a SiO_2 dielectric layer is deposited to form an overgrown mask. By using an inductively coupling plasma technique, the SiO_2 layer is dry etched to form regularly arrayed micro-holes (where the diameter and the spacing are $3.6 \mu\text{m}$

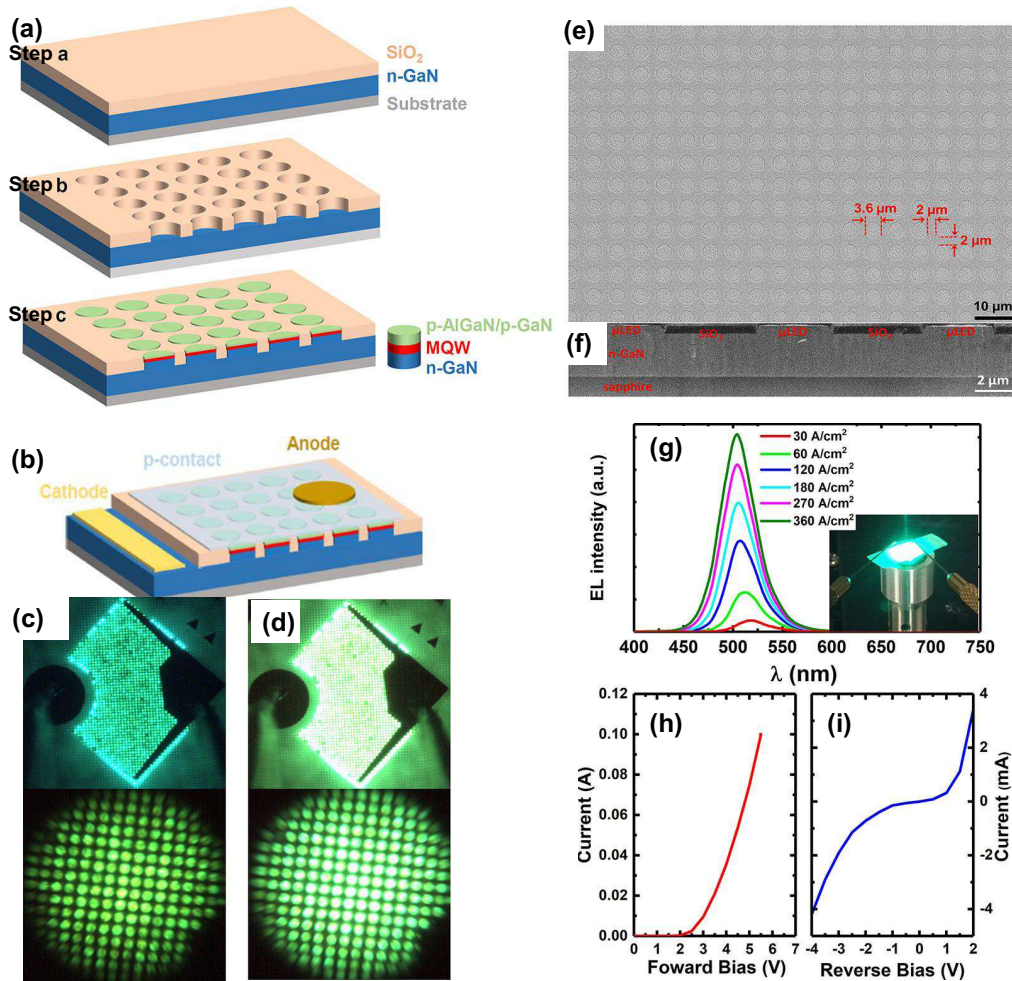


Fig. 1. (a) Procedures of our direct epitaxial approach; (b) LED device fabricated on overgrown μ LED arrays; (c) μ LED emission images at 3 A/cm^2 ; (d) μ LED emission images at 9 A/cm^2 ; (e) top and (f) cross-sectional view SEM images of our overgrown μ LEDs (diameter: $3.6 \mu\text{m}$, spacing: $2 \mu\text{m}$); (g) EL spectra, (h) I - V and (i) reverse leakage current of overgrown μ LEDs. Reprinted with permission from Ref. [33]. Copyright 2020 American Chemical Society (<https://creativecommons.org/licenses/by/4.0/>).

and 2 μm , respectively, both of which are able to be tuned according to specific applications), a standard LED structure is then selectively overgrown within the regularly arrayed micro-holes. The height of the final LED structure has to level with the mask thickness, ensuring that the selective epitaxial growth is entirely confined within the regularly arrayed micro-holes. Finally, regularly arrayed μLEDs are naturally formed without involving any dry-etching processes.^[33,34] A detailed procedure is provided in Ref. [33] and cited here in Fig. 1(a). The surface of the μLED wafer is flat as shown in Figs. 1(e) and 1(f). The micro-hole arrayed SiO_2 masks also serve as an insulation layer between individual μLEDs . A layer of indium-tin-oxide (ITO) covers all the p-GaN of μLED arrays and the anode metal is further deposited on it, forming a common-anode structure. For the fabrication of n-contact, the n-GaN is exposed by dry etching down to the n-GaN layer where Ti/Al alloys are deposited. The schematics of the μLEDs arrays, the light emission, the electro-luminescence (EL) spectra, the I - V and the reverse leakage current of μLEDs are shown in Figs. 1(b)–1(i), respectively. It can be seen that both the fabrication and the growth procedure are simple and straightforward and there is no need of planarization or filling with polymer or dielectrics.

3.2. Advantages of the CSE approach

Many advantages have been demonstrated by using the direct epitaxial approach to obtain μLEDs compared with any traditional dry-etching approaches in terms of EQE, emission wavelength stability, easiness to achieve long-wavelength emission (namely, red color), low reverse leakage current and potential to integrating with electronic devices.

3.2.1. High EQE and ultra-compact size

For AR/VR devices, μLEDs with a dimension of $\leq 5 \mu\text{m}$ are the key components. However, the EQE of the μLEDs with such a size range fabricated using conventional dry etching methods is generally limited to 1% to 5%,^[14] which cannot meet the requirements for AR/VR applications. This is mainly caused by severe damages on the sidewalls, which cannot be totally recovered by any sidewall passivation techniques. In contrast, our direct epitaxial approach does not have this issue.

Being different from the growth procedure in Subsection 3.1, a bottom nanoporous DBR structure was prepared prior to the growth of an n-GaN layer to improve the light extraction efficiency. The nanoporous DBR is formed by electrochemical (EC) etching the 11 pairs of alternating heavily-doped $\text{n}^{++}\text{-GaN}$ (doping level on an order of $> 5 \times 10^{19}/\text{cm}^3$) and undoped GaN layers beneath the n-GaN layer. The growth procedure and the EL characteristics of the device are demonstrated in Figs. 2(a)–2(e), showing that the peak EQE is 6% for the μLEDs without a bottom DBR and 9% for the μLEDs with a bottom DBR. It is worth noting that the light output power (LOP) and EQE are measured on a bare chip without any package or roughening as shown in Fig. 2(f). This high EQE has surpassed the results of 4%–5% achieved by the conventional dry etching method with an ALD oxide passivation for an efficiency remedy in Ref. [14]. This mainly attributes to the fact that in our approach dry etching is not needed anymore and thus there is no damage to sidewalls.^[33,34] Since the size and the spacing of μLEDs are solely determined by the diameters and the spacing of the regularly arrayed micro-hole masks, a μLED display with an ultrahigh definition and an ultra-small pixel size can be achieved by further scaling down the size of the micro-hole masks used for the direct epitaxial approach.

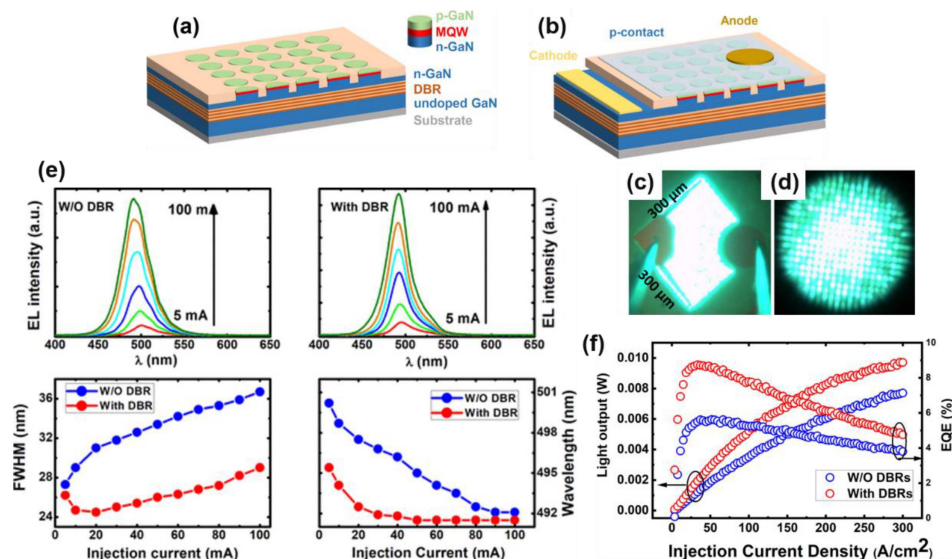


Fig. 2. (a) A schematic of overgrown μLEDs , (b) a LED device schematic, (c) and (d) light emission images at 15 A/cm^2 ; (e) EL spectra, peak wavelength and FWHM for μLEDs with and without DBR; (f) LOP and EQE of the μLED arrays with and without DBRs. Reprinted with permission from Ref. [34]. Copyright 2020 American Chemical Society (<https://creativecommons.org/licenses/by/4.0/>).

3.2.2. Demonstration of μ LEDs with excellent stabilization in emission wavelength

Emission wavelength instability with increasing injection current is a long-standing issue for III-nitride LEDs, which is caused by the well-known quantum confined Stark effect (QCSE) resulted from the inherent polarization fields in the InGaN/GaN multiple quantum well (MQW) region. It is also well-known that the wavelength of an optical mode formed in a microcavity is insensitive to the injection current. Therefore, this instability issue of the emission wavelength of III-nitride LEDs can be resolved if a proper structure can be designed so that it allows the emission from the LED to be coupled with an optical mode via a microcavity. By means of employing a nanoporous bottom DBR structure consisting of n^{++} GaN/u-GaN layers (the same DBR structure used in Subsection 3.2.1) and a top dielectric DBR structure, a proper microcavity structure (designed via a simulation method) can generate a strong coupling between the emission of μ LEDs and the optical modes via the microcavity. Based on this idea, excellent stabilization in emission wavelength has been

achieved as shown in Fig. 3, indicating that the emission wavelength of our μ LEDs with a strong coupling between the emission of μ LEDs and the optical modes via a properly designed microcavity is stable at 520 nm with increasing current from 5 mA to 60 mA, while the μ LEDs without any DBR structure show a wavelength shift from 560 nm to 510 nm under identical measurement conditions. Based on a detailed simulation, the optical modes in the green spectral region have been clearly identified. Generally speaking, the wavelength of an optical mode formed in a microcavity is mainly determined by the length and the refractive index of the microcavity instead of the injection current. Therefore, if the light emission from the μ LEDs can be coupled with the optical modes via the microcavity, the emission from the μ LEDs can obtain the properties of the optical modes and thus the emission wavelength tends to become stabilized.^[35] A very clear mode at 480 nm and 526 nm can be observed from the simulation as shown in Fig. 3, confirming the existence of the optical modes in the μ LED structure.

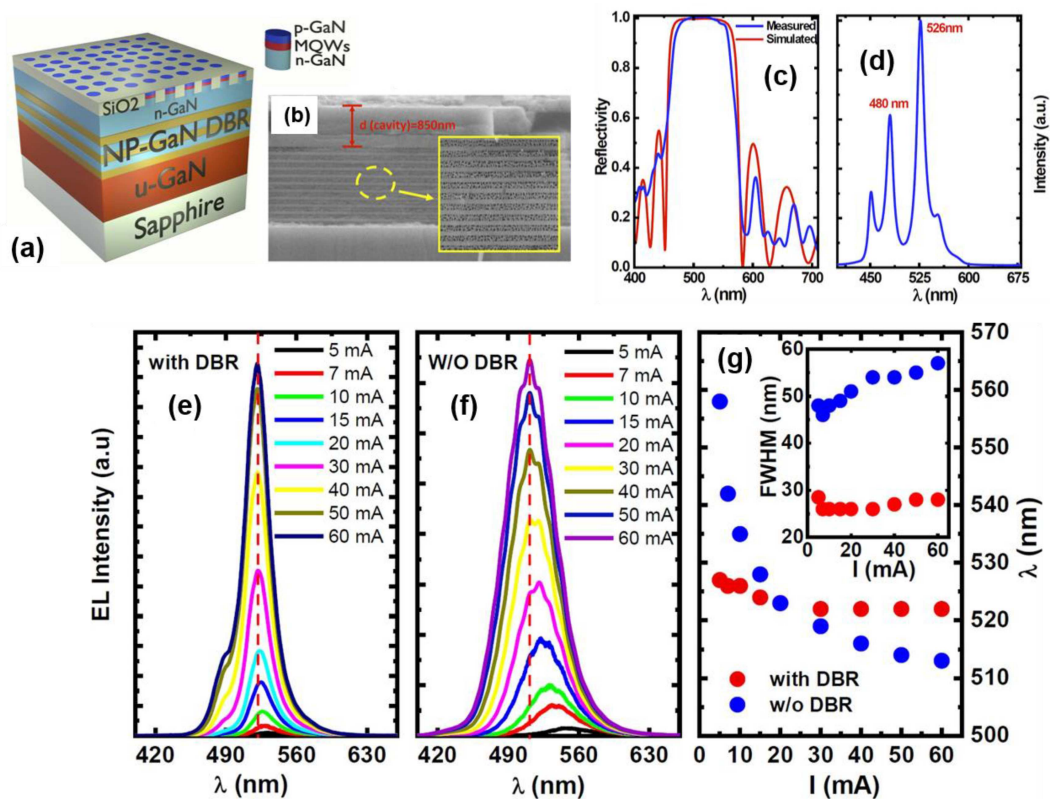


Fig. 3. (a) A schematic of overgrown μ LEDs with a nanoporous DBR at the bottom; (b) cross-sectional SEM images after electrochemical etching, forming 11 pairs of nanoporous-GaN/undoped GaN DBR; (c) measured and simulated reflectance spectrum of nanoporous GaN DBR; (d) mode spectrum simulated by 3D FDTD software; (e) EL spectra of μ LEDs with a bottom DBR and (f) without a bottom DBR; (g) peak wavelength and full width half maximum of two types of μ LEDs. Reprinted with permission from Ref. [35]. Copyright 2022 American Chemical Society (<https://creativecommons.org/licenses/by/4.0/>).

3.2.3. Demonstration of red μ LEDs due to enhanced indium incorporation

To achieve red emission, AlGaInP materials are normally adopted. However, AlGaInP is not the best choice for the fabrication of μ LEDs due to its high surface recombination

rate and long carrier diffusion length, resulting in much more serious nonradiative recombination and thus lower efficiency than its InGaIn counterparts. On the other side, InGaIn-based red μ LEDs share the same materials as blue and green LEDs, making it much favorable to integrate RGB for the fabrication

of full-color displays than that obtained by mixing III-nitrides and AlInGaP.

Currently, III-nitride based red μ LEDs are generally achieved by inserting AlN or AlGaP layers underneath quantum wells aiming to obtain strain relaxation for enhancing indium incorporation into GaN.^[40–43] This is also the reason that it is more favorable to choose silicon substrates for the growth of red LEDs (tensile strain) than sapphire substrates (compressive strain). However, this method always introduces extra defects thus deteriorating internal quantum efficiency. In our di-

rect epitaxial approach, μ LEDs are grown in the regularly arrayed micro-holes, naturally forming relaxation in the lateral direction and thus enhancing indium incorporation into GaN. Using regularly arrayed micro-hole masks (namely, 2 μ m diameter and 1.5 μ m-spacing), red μ LEDs with an emission wavelength at 642 nm and a peak EQE of 1.75% have been achieved,^[36] as shown in Fig. 4. For a comparison, a planar LED (labeled as LED B) was grown in the same run, but only green emission was achieved, proving that our direct epitaxial approach also favors obtaining a longer emission wavelength.

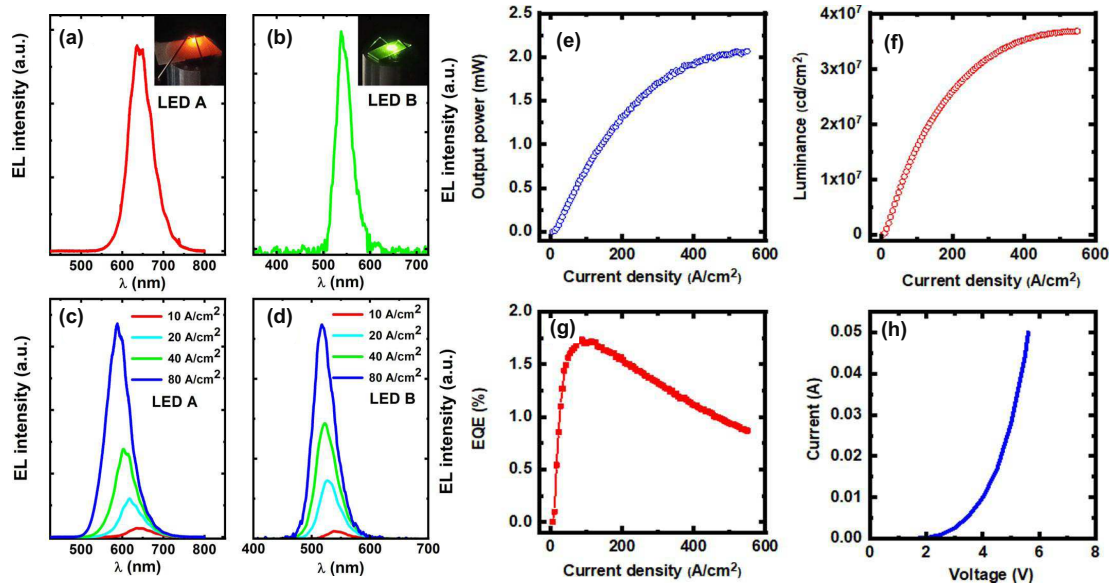


Fig. 4. EL spectra at 10 A/cm² for (a) overgrown μ LED arrays (LED A) and (b) planar reference (LED B) and insets are emission images. EL spectra with increased current densities from 10 A/cm² to 80 A/cm² for (c) LED A and (d) LED B, respectively; (e) light output power, (f) luminance, (g) EQE, and (h) current–voltage characteristics of the μ LED array device (LED A). Reprinted with permission from Ref. [36]. Copyright 2022 American Chemical Society (<https://creativecommons.org/licenses/by/4.0/>).

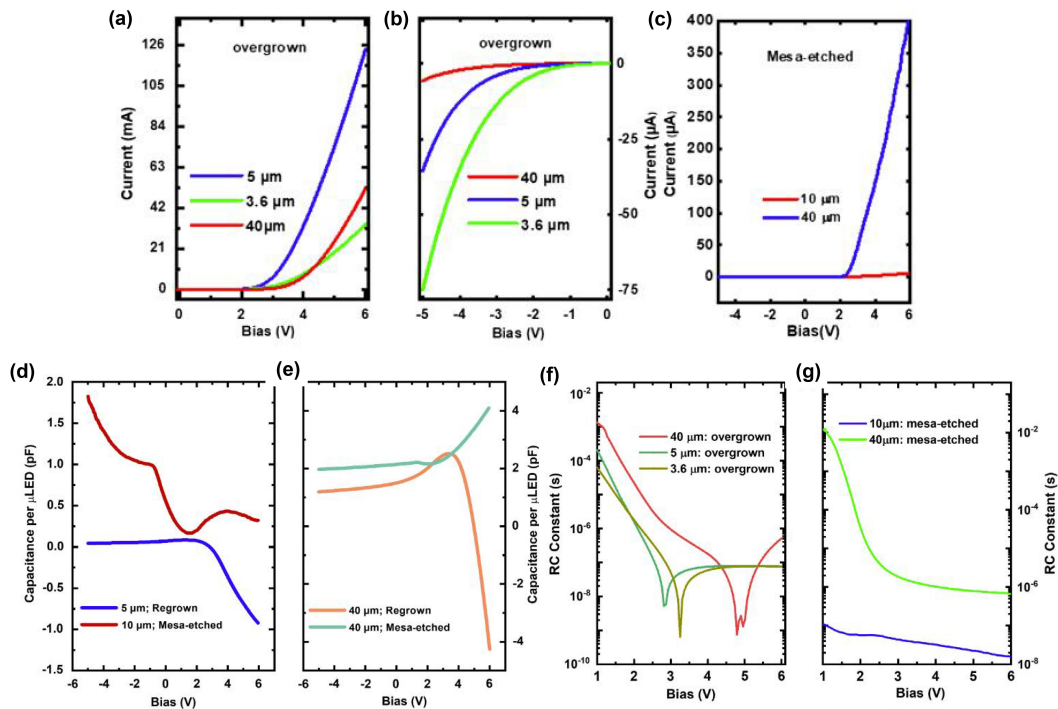


Fig. 5. (a) Forward I - V characteristics of three overgrown μ LEDs (diameter: 3.6 μ m, 5 μ m and 40 μ m); (b) reverse leakage current; (c) I - V characteristics for μ LEDs with conventional etching methods; (d) and (e) capacitance comparison of overgrown μ LEDs and mesa-etched ones; (f) and (g) RC constants comparison between overgrown μ LEDs and mesa-etched ones. Reprinted with permission from Ref. [37]. Copyright 2021 Phys. Status Solidi A/Wiley-VCH (<https://creativecommons.org/licenses/by/4.0/>).

3.2.4. Demonstration of μ LEDs with reduced leakage current

Leakage current is a particularly serious issue for μ LEDs, as it often generates an unintentional switch-on of pixels in practical applications. Many reasons can cause leakage current including surface recombination and sidewall damage induced as a result of dry etching. Of course, it also leads to reduced luminous efficiency. Our direct epitaxial approach does not suffer from side wall damages, leading to a great potential to reduce the reverse leakage current. To confirm this, a comparative measurement using LCR meter and Keithley power source has been carried out to investigate the current–voltage (I – V) and capacitance–voltage (C – V) performances of the μ LEDs fabricated using a conventional dry etching approach and our direct epitaxial approach. By measuring the leakage current of the μ LEDs achieved by our direct approach, it was found that the leakage current per μ LED and the leakage current dispersion are smaller than those of the conventionally mesa-etched μ LEDs. With reducing the size of μ LEDs, leakage current increases due to an increased perimeter to area ratio and corresponding larger surface recombination rate. Reduced leakage current can ensure high luminous efficiency

with scaling down μ LED size. By measuring capacitance–voltage behaviors, it was found that both operational voltage and RC constants show more favorable to the devices obtained by using our direct epitaxial approach than the conventionally mesa-etched μ LEDs^[37] as shown in Fig. 5. This feature makes the μ LEDs obtained using our direct epitaxial approach suitable for high-speed switching applications such as VLC.

4. Demonstration of a monolithic integration of μ LEDs with HEMTs for microdisplay and VLC

Microdisplay can only work with its electronic driving parts. Therefore, it is also important to integrate μ LEDs with its electronic driving circuits. Currently, a heterogeneous integration approach is widely adopted, such as wafer-to-wafer bonding to integrate μ LED display with CMOS circuits for AR applications and mass transfer (laser lift-off, pick and place, etc.) to integrate μ LED chips with TFT backplane for TV applications. However, high cost, low yield and poor assembly efficiency are still hindering these techniques being employed in massive production.

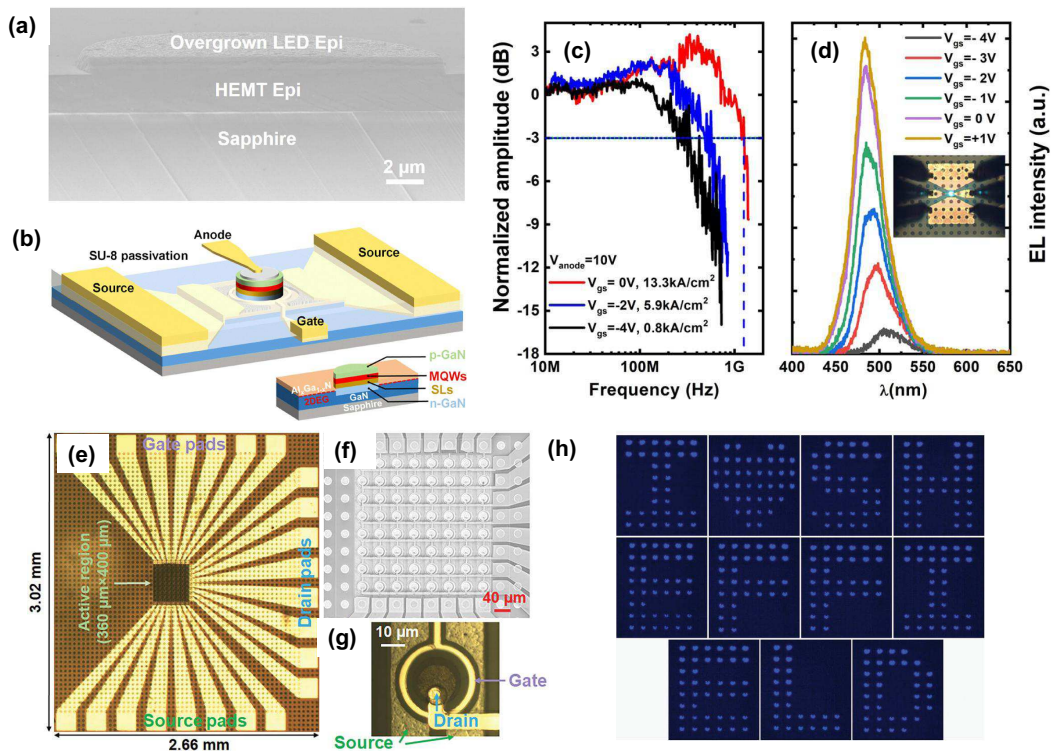


Fig. 6. (a) A cross-sectional SEM image and (b) schematic illustration of single monolithic HEMT- μ LED device; (c) 3 dB bandwidth and (d) EL spectra of integrated devices;^[38] (e) 8×8 HEMT- μ LED arrays as a display chip; (f) an SEM image of active region and (g) a single pixel microscopic image and (h) displayed images. Reprinted with permission from Ref. [38] Copyright 2021 American Chemical Society and Ref. [39] 2021 Advanced Materials Technologies/Wiley-VCH (<https://creativecommons.org/licenses/by/4.0/>).

In contrast, our direct epitaxial approach can also enable a monolithic integration of μ LEDs with HEMTs. Traditional selective overgrowth method suffers from etching damage to LEDs and largely an increased growth rate near the boundary

between mask covered region and overgrowth region.^[44–48] Here, in our approach, a proper design in growth parameter ensures a uniform growth rate across the whole region, thus leading to smooth surface of μ LEDs. For our direct epitaxy ap-

proach, there is no etching process involved, eliminating dry-etching induced damages on the sidewalls of μ LEDs. By using our direct epitaxial approach on a HEMT template, we have successfully demonstrated a monolithic HEMT- μ LED device (where the μ LEDs diameter is 20 μ m) with a 1.2 GHz 3 dB-bandwidth as shown in Figs. 6(a)–6(d),^[38] the highest one reported for c-plane III-nitride LEDs.^[49]

Furthermore, an 8×8 monolithically integrated HEMT- μ LED arrays have been achieved^[39] as shown in Figs. 6(e)–6(h), demonstrating a new concept for microdisplay applications. Such a monolithic integration scheme avoids the great difficulty in employing either the widely used mass transfer approach or the pick-and-place method for assembly.

5. Conclusion and perspectives

In summary, a confined selective epitaxy approach to achieving μ LEDs has been developed by the Sheffield team, featuring many major advantages such as ultrahigh external quantum efficiency, stable emission color, enhanced indium incorporation to achieve red emissions, low leakage current and parasitic capacitance, and great potential to be integrated with electronic devices. All these advantages make this approach a promising candidate to fabricate high quality μ LEDs for microdisplay and VLC applications.

Acknowledgment

Project supported by the Engineering and Physical Sciences Research Council (EPSRC), U.K., via EP/P006973/1, EP/T013001/1, and EP/M015181/1.

References

- [1] Lee V W, Twu N and Kymissis I 2016 *J. Inf. Disp.* **32** 16
- [2] Fan Z Y, Lin J Y and Jiang H X 2008 *J. Phys. D* **41** 094001
- [3] Templier F 2016 *J. Soc. Inf. Disp.* **24** 669
- [4] Day J, Li J, Lie D Y C, Bradford C, Lin J Y and Jiang H X 2011 *Appl. Phys. Lett.* **99** 031116
- [5] Green R P, McKendry J J D, Massoubre D, Gu E, Dawson M D and Kelly A E 2013 *Appl. Phys. Lett.* **102** 091103
- [6] Rajbhandari S, McKendry J J D, Herrnsdorf J, Chun H, Faulkner G, Haas H, Watson I M, O'Brien D and Dawson M D 2017 *Semicond. Sci. Technol.* **32** 023001
- [7] Ozden I, Diagne M, Nurmikko A V, Han J and Takeuchi T 2001 *Phys. Status Solidi A* **188** 139
- [8] Liu Z J, Wong K M, Keung C W, Tang C W and Lau K M 2009 *IEEE J. Sel. Top. Quantum Electron.* **15** 4
- [9] Otto I, Mounir C, Nirschl A, Pfeuffer A, Schapers Th, Schwarz U T and von Malm N 2015 *Appl. Phys. Lett.* **106** 151108
- [10] Li K H, Cheung Y F, Tang C W, Zhao C, Lau K M and Choi H W 2016 *Phys. Status Solidi A* **213** 5
- [11] Templier F, Dupre L, Tirano S, Marra M, Verney V, Olivier F, Avenirur B, Sarasin D, Marion F, Catelain T, Berger F, Mathieu L, Dupont B and Gamarra P 2016 *Dig. Tech. Pap.-Soc. Inf. Disp. Int. Symp.* **47** 1013
- [12] Ploch N L, Rodriguez H, Stölmackerr C, Hoppe M, Lapeyrade M, Stellmach J, Mehnke, F, Wernicke T, Knauer A, Kueller V, Weyers M, Einfeldt S and Kneissl M 2013 *IEEE Trans. Electron Devices* **60** 782
- [13] Olivier F, Daami A, Licitra C and Templier F 2017 *Appl. Phys. Lett.* **111** 022104
- [14] Wong M S, Hwang D, Alhassan A I, Lee C, Ley R, Nakamura S and DenBaars S P 2018 *Opt. Express* **26** 21324
- [15] Konoplev S S, Bulashevich K A and Karpov S Y 2018 *Phys. Status Solidi A* **215** 1700508
- [16] Yang C M, Kim D S, Park Y S, Lee J H, Lee Y S and Lee J H 2012 *Opt. Photonics J.* **2** 185
- [17] Zhang Y, Guo Y, Li Z, Wei T, Li J, Yi X and Wang G 2012 *IEEE Photonics Technol. Lett.* **24** 4
- [18] Zuo P, Zhao B, Yan S, Yue G, Yang H, Li Y, Wu H, Jiang Y, Jia H, Zhou J and Chen H 2016 *Opt. Quantum Electron.* **48** 1
- [19] Hwang D, Mughal A, Pynn C D, Nakamura S and DenBaars S P 2017 *Appl. Phys. Express* **10** 032101
- [20] Templier F, Benaïssa L, Avenirur B, Nardo C D, Charles M, Daami A, Henry F and Dupre L 2017 *Dig. Tech. Pap. - Soc. Inf. Disp. Int. Symp.* **48** 268
- [21] El-Masry N A, Piner E L, Liu S X and Bedair S M 1998 *Appl. Phys. Lett.* **72** 40
- [22] Wakahara A, Tokuda T, Dang X Z, Noda S and Sasaki A 1997 *Appl. Phys. Lett.* **71** 906
- [23] Inatomi Y, Kanagawa Y, Ito T and Suski T 2017 *Jpn. J. Appl. Phys.* **56** 078003
- [24] Wang T 2016 *Semicond. Sci. Technol.* **31** 093003
- [25] Pereira S, Correia M R, Pereira E, O'Donnell K P, Alves E, Sequeira A D, Franco N, Watson I M and Deatcher C J 2002 *Appl. Phys. Lett.* **80** 3913
- [26] Shimizu M, Kawaguchi Y, Hiramatsu K and Sawaki N 1997 *Jpn. J. Appl. Phys.* **36** 3381
- [27] Sonderegger S, Feltin E, Merano M, Crottini A, Carlin J F, Sachot R, Deveaud B, Grandjean N and Ganiere J D 2006 *Appl. Phys. Lett.* **89** 232109
- [28] Tawfik W Z, Hyun G Y, Ryu S W, Ha J S and Lee J K 2016 *Opt. Mater.* **55** 17
- [29] Iida D, Zhuang Z, Kirilenko P, Velazquez-Rizo M, Najmi M A and Ohkawaa K 2020 *Appl. Phys. Lett.* **116** 162101
- [30] Hwang J I, Hashimoto R, Saito S and Nunoue S 2014 *Appl. Phys. Express* **7** 071003
- [31] Hashimoto R, Hwang J, Saito S and Nunoue S 2014 *Phys. Status Solidi C* **11** 628
- [32] Zhuang Z, Iida D and Ohkawa K 2022 *Jpn. J. Appl. Phys.* **61** SA0809
- [33] Bai J, Cai Y, Feng P, Fletcher P, Zhao X, Zhu C and Wang T 2020 *ACS Photonics* **7** 411
- [34] Bai J, Cai Y, Feng P, Fletcher P, Zhu C, Tian Y and Wang T 2020 *ACS Nano* **14** 6906
- [35] Martinez de Arriba G, Feng P, Xu C, Zhu C, Bai J and Wang T 2022 *ACS Photonics* **9** 2073
- [36] Feng P, Xu C, Bai J, Zhu C, Farrer I, Martinez de Arriba G and Wang T 2022 *ACS Appl. Electron. Mater.* **4** 2787
- [37] Esendag V, Bai J, Fletcher P, Feng P, Zhu C, Cai Y and Wang T 2021 *Physica Status Solidi A* **218** 2100474
- [38] Cai Y, Haggag J I H, Zhu C, Feng P, Bai J and Wang T 2021 *ACS Appl. Electron. Mater.* **3** 445
- [39] Cai Y, Zhu C, Zhong W, Feng P, Jiang S and Wang T 2021 *Adv. Mater. Technol.* **6** 2100214
- [40] Li P, Li H, Yang Y, Zhang H, Shapturenka P, Wong M, Lynsky C, Iza M, Gordon M J, Speck J S, Nakamura S and DenBaars S P 2022 *Appl. Phys. Lett.* **120** 041102
- [41] Li P, Li H, Zhang H, Yang Y, Wong M S, Lynsky C, Iza M, Gordon M J, Speck J S, Nakamura S and DenBaars S P 2022 *Appl. Phys. Lett.* **120** 121102
- [42] Horng R H, Ye C X, Chen P W, Iida D, Ohkawa K, Wu Y R and Wu D S 2022 *Sci. Rep.* **12** 1324
- [43] Yu L, Wang L, Yang P, Hao Z, Yu J, Luo Y, Sun C, Xiong B, Han Y, Wang J, Li H and Wang L 2022 *Opt. Mater. Express* **12** 3225
- [44] Li Z, Waldron J, Detchprohm T, Wetzel C, Karlick Jr R F and Chow T P 2013 *Appl. Phys. Lett.* **102** 192107
- [45] Liu Z, Huang T, Ma J, Liu C and Lau K M 2014 *IEEE Electron Device Lett.* **35** 330
- [46] Liu Z, Ma J, Huang T, Liu C and Lau K M 2014 *Appl. Phys. Lett.* **104** 091103
- [47] Liu C, Cai Y, Liu Z, Ma J and Lau K M 2015 *Appl. Phys. Lett.* **106** 181110
- [48] Cai Y, Zou X, Liu C and Lau K M 2017 *IEEE Electron Device Lett.* **39** 224
- [49] Yu L, Wang L, Hao Z, Luo Y, Sun C, Xiong B, Han Y, Wang J and Li H 2022 *Semicond. Sci. Technol.* **37** 023001